IVYSPRING INTERNATIONAL PUBLISHER

International Journal of Medical Sciences

2026; 23(12): 3806-3821. doi: 10.7150/ijms.139201

Research Paper

Pre-ablation substrate phenotypes and recurrence after atrial fibrillation catheter ablation: a retrospective cohort study

Zixi Zhang, MD[1], Jiaxin Chi, MD[1], Xunhua Wang, MD[1], Xiaoyu Zeng, MD[1], Haoqing Yu, MD[1], Siyuan Tan, MD[1], Ke Hu, MD[1], Yichao Xiao, MD[1], Tao Tu, MD[1], Kangrong Li, MD[1], Qiuzhen Lin, MD[1], Qiming Liu, MD[1], Yongguo Dai, Ph.D.[2,✉], Chan Liu, Ph.D.[3,✉]

1. Department of Cardiology, The Second Xiangya Hospital, Central South University, Changsha City, Hunan Province, People's Republic of China.
2. Department of Pharmacy, Xiangya Hospital, Central South University; National Clinical Research Center for Geriatric Diseases (Xiangya Hospital of Central South University), Changsha City, Hunan Province, People's Republic of China.
3. Department of International Medicine, The Second Xiangya Hospital, Central South University, Changsha City, Hunan Province, People's Republic of China.

✉ Corresponding authors: Chan Liu, Ph.D. Department of International Medicine, The Second Xiangya Hospital, Central South University. Address: 139 Renmin Road, Furong District, Changsha City, Hunan Province, People's Republic of China. E-mail: liuchan6390@csu.edu.cn. Yongguo Dai, Ph.D. Department of Pharmacy, Xiangya Hospital, Central South University. Address: 87 Xiangya Road, Kaifu District, Changsha City, Hunan Province, People's Republic of China. E-mail: daiyongguo1995@csu.edu.cn.

© 2026 The Author(s). This is an open access article distributed under the Creative Commons Attribution 4.0 International Licence, subject to the Publisher's Terms of Use at https://ivyspring.com/terms.

Received: 2026.06.11; Accepted: 2026.11.04; Published: 2026.11.13

Abstract

Background: Recurrence after atrial fibrillation (AF) catheter ablation may reflect heterogeneity in atrial and systemic substrate burden. We investigated the temporal reproducibility of outcome-independent multidomain pre-ablation phenotypes, their associations with recurrence, and their incremental prognostic value.

Methods: This retrospective cohort included 1654 patients undergoing first-time AF ablation. Partitioning around medoids clustering with domain-balanced Gower distance integrated 17 pre-ablation variables across six domains. Cox regression evaluated early recurrence within 3 months in the full cohort and post-blanking recurrence by 12 months and during follow-up in the 3-month landmark cohort (n = 1552). Stability, temporal reproducibility, continuous substrate-position associations, and incremental prediction were evaluated.

Results: Clustering identified a lower systemic-burden phenotype (n = 772) and a higher cardiometabolic-inflammatory phenotype (n = 882). The latter had greater cardiometabolic and inflammatory-nutritional burden, larger left atrial diameter, and reduced renal function. It was associated with post-blanking recurrence by 12 months [adjusted hazard ratio (HR): 3.47, 95% confidence interval (CI): 2.54–4.75] and during follow-up (HR: 2.85, 95% CI: 2.28–3.56), but not significantly with early recurrence (HR: 1.19, 95% CI: 0.80–1.79). Internal temporal validation showed substantial agreement between frozen assignments and independently derived clusters (adjusted Rand index: 0.775; agreement: 94.0%). The continuous score was nonlinearly associated with recurrence. Adding phenotype membership to a clinical benchmark model increased the apparent time-dependent area under the receiver operating characteristic curve from 0.6941 to 0.7068, although incremental discrimination varied across out-of-bag bootstrap evaluations.

Conclusions: Multidomain phenotyping identified pre-ablation profiles associated with post-blanking recurrence that demonstrated internal stability and temporal reproducibility.

Keywords: atrial fibrillation; catheter ablation; arrhythmia recurrence; substrate phenotyping; unsupervised clustering; cardiometabolic burden

1. Introduction

Atrial fibrillation (AF) is the most common sustained cardiac arrhythmia and is associated with increased risks of stroke and heart failure, impaired quality of life, and greater healthcare utilization [1-3]. Its prevalence continues to rise alongside population aging and the growing burden of cardiometabolic

disease [4]. These conditions contribute to atrial remodeling through interacting hemodynamic, metabolic, inflammatory, renal, and neurohormonal mechanisms, underscoring the heterogeneous atrial and systemic substrates involved in AF beyond electrical triggers alone [5, 6].

Catheter ablation is an established rhythm-control strategy for selected patients with AF, with pulmonary vein isolation remaining the cornerstone of contemporary practice [7]. Advances in electroanatomic mapping, energy delivery, lesion assessment, and periprocedural care have shaped contemporary AF ablation practice [8]. Nevertheless, post-ablation recurrence remains common, with considerable variation in outcomes among patients. Although pulmonary vein reconnection, non-pulmonary vein triggers, and lesion-related factors contribute to recurrence, patients undergoing comparable ablation procedures may experience substantially different clinical trajectories [6]. This variability suggests that pre-existing atrial and systemic substrate characteristics may contribute to differences in rhythm-control outcomes.

Previous studies have identified several factors associated with AF recurrence after ablation, including AF type, left atrial remodeling, cardiometabolic comorbidities, systemic inflammation, renal dysfunction, and markers of myocardial stress [9-12]. Established clinical risk scores, including APPLE and CAAP-AF, combine prespecified clinical predictors to estimate recurrence risk, although their prognostic performance has varied across studies [13-15]. Beyond conventional risk modeling, unsupervised clustering offers an approach to characterizing patterns of coexisting abnormalities without using subsequent clinical outcomes to define patient groups. Previous research has identified distinct clinical phenotypes associated with recurrence after AF ablation using unsupervised cluster analysis [16]. However, the temporal reproducibility of multidomain substrate phenotypes and their incremental prognostic performance beyond established clinical predictors remain insufficiently characterized.

Because atrial and systemic substrate abnormalities may vary along overlapping multidimensional continua, phenotype classification may provide a simplified representation of underlying clinical heterogeneity. In this retrospective cohort of patients undergoing first-time AF catheter ablation, we therefore used routinely available pre-ablation variables to derive multidomain substrate phenotypes and examined their associations with early and post-blanking recurrence. We assessed the internal stability and temporal reproducibility of phenotype assignments and explored the relationship between binary phenotype membership and a continuous substrate-position score. We separately evaluated whether these representations improved prognostic discrimination, calibration, and decision-analytic utility beyond established clinical predictors. Our primary objective was to characterize multidomain pre-ablation substrate heterogeneity and its association with recurrence, while distinguishing phenotypic characterization from incremental prognostic performance.

2. Methods

2.1 Study design and population

This single-center retrospective cohort study was conducted in the Department of Cardiology at The Second Xiangya Hospital, Central South University. Adults aged ≥ 18 years who underwent catheter ablation for AF between December 2009 and December 2024 were screened for eligibility.

Patients were excluded if they had acute heart failure or hemodynamic instability, severe valvular heart disease requiring intervention, acute myocardial infarction, severe hepatic or renal dysfunction, clinically significant endocrine disorders affecting cardiometabolic or hemodynamic status, active malignancy, active infection, systemic autoimmune disease, previous AF catheter ablation, pregnancy, or insufficient clinical, laboratory, procedural, or follow-up data required for the prespecified analyses. After applying these criteria, 1654 patients were included in the final analytical cohort. The study selection process is shown in Figure 1, and detailed exclusion criteria are provided in Supplementary Method 1.

The study was conducted in accordance with the Declaration of Helsinki and was approved by the Biomedical Research Ethics Committee of The Second Xiangya Hospital, Central South University (LYEC2026-0047). The requirement for written informed consent was waived because of the retrospective design and use of de-identified data.

2.2 Data collection and variable definitions

Pre-ablation clinical data were extracted from the hospital information system using a standardized collection form. Two trained investigators independently extracted the data while blinded to recurrence status. Discrepancies were reviewed by a third investigator and resolved by verification against the original medical records.

Demographic and clinical variables included age, sex, body mass index (BMI), AF type, smoking status, alcohol consumption, hypertension, diabetes mellitus, dyslipidemia, coronary heart disease, heart failure, and obstructive sleep apnea. AF was classified as

paroxysmal or persistent according to established clinical definitions [7, 8]. Comorbidities were ascertained from documented medical histories, discharge diagnoses, clinical assessments, laboratory results, and medication records.

Anthropometric measurements were obtained as part of routine pre-ablation assessment. Echocardiographic variables included left atrial diameter (LAD) and left ventricular ejection fraction (LVEF). LVEF was assessed using the modified biplane Simpson method, whereas LAD was measured according to institutional echocardiographic protocols [17]. All echocardiographic examinations were performed by experienced cardiac sonographers.

Laboratory measurements included glycated hemoglobin (HbA1c), triglycerides, C-reactive protein (CRP), serum albumin, estimated glomerular filtration rate (eGFR), uric acid, and N-terminal pro-B-type natriuretic peptide (NT-proBNP). Fasting venous blood samples were collected before ablation and analyzed in the hospital's central laboratory using standardized procedures.

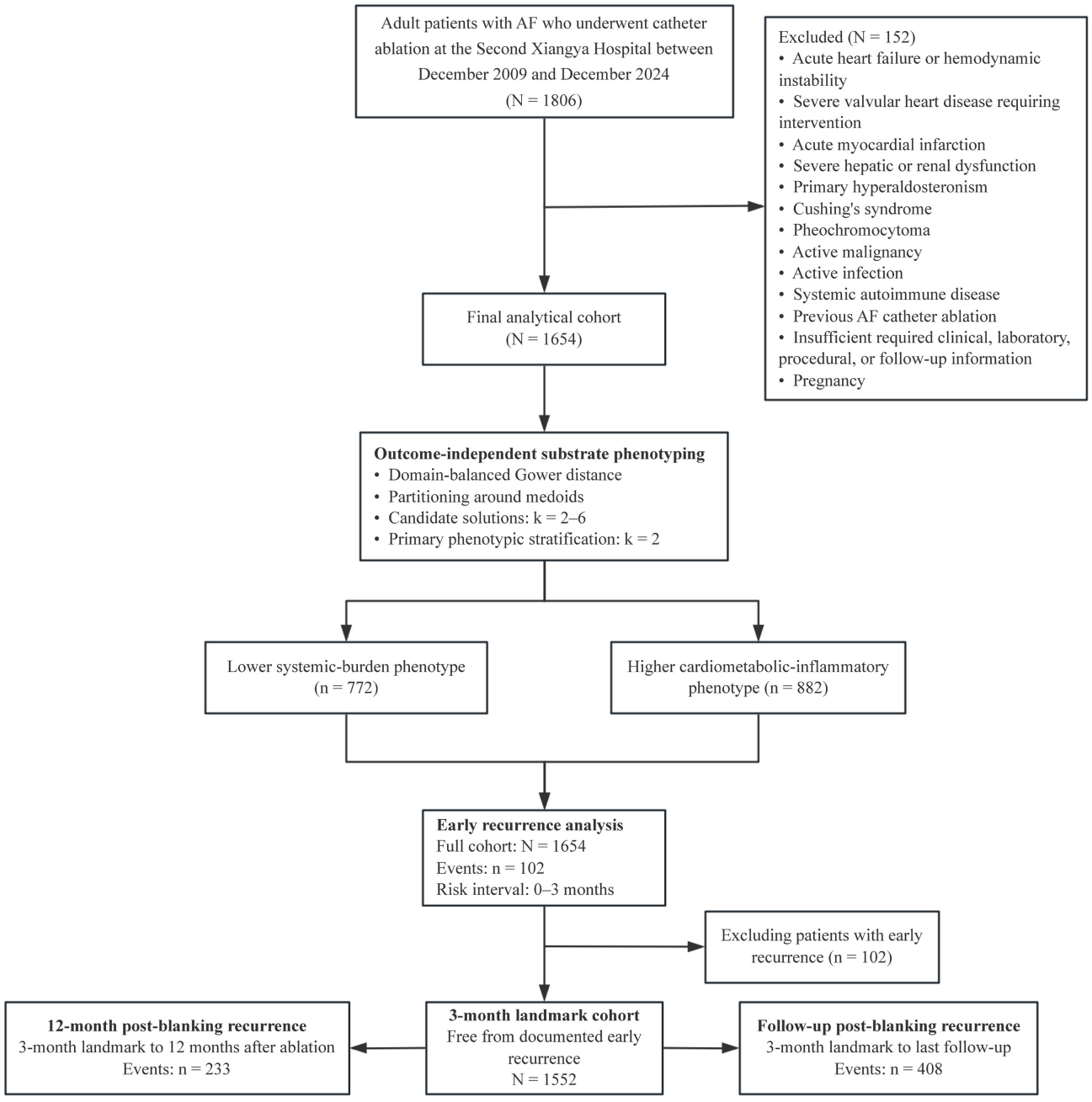


Figure 1. Study flowchart and outcome-specific analytical populations. Abbreviations: AF, atrial fibrillation.

Pre-ablation medication use included statins, β-blockers, angiotensin-converting enzyme inhibitors (ACEIs) or angiotensin receptor blockers (ARBs), angiotensin receptor–neprilysin inhibitors (ARNIs), vitamin K antagonists (VKAs), non-vitamin K antagonist oral anticoagulants (NOACs), amiodarone, and dronedarone. Procedural data included the date of the index ablation and ablation modality, categorized as radiofrequency ablation (RFA), cryoballoon ablation (CBA), or pulsed field ablation (PFA).

2.3 Ablation procedure, periprocedural management, and follow-up

Preprocedural evaluation and periprocedural management followed institutional protocols and clinical practices in effect at the time of treatment. International AF management guidelines and expert consensus statements provided the framework for procedural definitions and reporting [7, 8]. Preprocedural imaging was performed, as clinically indicated, to evaluate left atrial and pulmonary venous anatomy and exclude left atrial thrombus. Thromboembolic and bleeding risks were assessed using the CHA_2DS_2-VASc and HAS-BLED scores, respectively. Periprocedural anticoagulation was individualized according to thromboembolic and bleeding risks, renal function, anticoagulant type, and procedural considerations.

Pulmonary vein isolation was the principal procedural endpoint. RFA, CBA, and PFA were performed according to institutional protocols and clinical practices applicable during the corresponding calendar period. Ablation modality was selected based on patient characteristics, procedural indications, operator judgment, and technology availability. Additional ablation beyond pulmonary vein isolation was performed when clinically indicated. All procedures were performed by experienced electrophysiologists.

After ablation, patients received standard postprocedural monitoring and medical therapy. Oral anticoagulation was continued for at least 2 months, with subsequent treatment guided by thromboembolic and bleeding risks and clinical assessment [7, 8]. Antiarrhythmic drugs were generally continued during the 3-month blanking period, with subsequent adjustments based on rhythm status, symptoms, and physician judgment.

Follow-up was scheduled at 3, 6, 9, and 12 months after ablation and at 6-month intervals thereafter. Assessments were conducted through outpatient visits, telephone interviews, or WeChat-based communication. At each contact, symptoms suggestive of atrial tachyarrhythmia, interval medical encounters, rhythm status, medication use, and postprocedural complications were reviewed. Patients reporting potentially arrhythmia-related symptoms were advised to undergo electrocardiographic evaluation at the study center or a local healthcare facility. Continuous electrocardiographic monitoring or implantable loop recorder surveillance was not routinely mandated during follow-up.

2.4 Outcomes

Recurrence was defined as objectively documented AF, atrial flutter, or atrial tachycardia lasting ≥ 30 seconds after catheter ablation [18]. A 3-month blanking period was used to maintain consistency with the historical study period and definitions established in earlier AF ablation consensus statements [18].

The primary outcome was follow-up post-blanking recurrence, defined as the first documented atrial tachyarrhythmia occurring after the 3-month landmark among patients without documented early recurrence who remained under follow-up at that landmark. Secondary outcomes were early recurrence within 3 months and post-blanking recurrence by 12 months after ablation. Early recurrence was defined as the first documented recurrence from the index procedure through 3 months after ablation. Post-blanking recurrence by 12 months was defined as the first documented recurrence occurring after the 3-month landmark and no later than 12 months after the index procedure.

For early recurrence, follow-up began on the date of ablation and ended at the first documented recurrence, 3 months after ablation, or the last available follow-up, whichever occurred first. Post-blanking analyses were restricted to patients without documented early recurrence who remained under follow-up at the 3-month landmark. For these analyses, follow-up time was calculated from the landmark to the first documented recurrence or censoring. For the 12-month outcome, follow-up ended at the first documented recurrence, 12 months after ablation, or the last available follow-up, whichever occurred first. For the primary outcome, follow-up continued until the first documented recurrence or the last available follow-up.

2.5 Substrate phenotyping and internal temporal validation

Seventeen pre-ablation variables were selected for phenotype derivation based on clinical relevance, routine availability, and representation of substrate-related pathophysiological domains. These variables included age, BMI, LAD, LVEF, hypertension, diabetes mellitus, dyslipidemia, coronary heart disease, heart

failure, obstructive sleep apnea, HbA1c, triglycerides, CRP, albumin, eGFR, uric acid, and NT-proBNP. Triglycerides, CRP, and NT-proBNP were transformed using log(1 + x) to reduce right-skewness. Recurrence outcomes were not used for variable selection, distance calculation, clustering, or phenotype assignment.

Pairwise dissimilarities were calculated using domain-balanced Gower distance to accommodate both continuous and categorical variables. The 17 variables were grouped into six prespecified clinical domains: cardiometabolic substrate, inflammatory-nutritional status, renal-metabolic status, atrial structural substrate, myocardial stress-functional status, and systemic comorbidity. Each domain was assigned equal total weight, with equal weighting of variables within each domain, to prevent domains containing more variables from disproportionately influencing phenotype assignment. Variable allocation and weighting are detailed in Supplementary Method 2.

Partitioning around medoids (PAM) clustering was applied to the weighted Gower distance matrix. Candidate solutions with k = 2–6 were evaluated according to average silhouette width, cluster sizes, parsimony, and clinical interpretability. The k = 2 solution was selected because it yielded the highest average silhouette width. The modest degree of cluster separation indicated that the resulting partition represented overlapping clinical profiles within a multidimensional distribution of substrate burden. Phenotype labels were assigned after clustering according to the observed clinical profiles and designated as the lower systemic-burden phenotype and the higher cardiometabolic-inflammatory phenotype.

Principal coordinates analysis (PCoA) was used to visualize patient distributions in the weighted Gower distance space. Between-phenotype differences in individual variables were quantified using standardized mean differences, and domain-level separation was summarized by the mean absolute standardized difference across variables within each domain. Internal clustering stability was assessed through 500 repeated subsampling iterations, each comprising 80% of the analytical cohort sampled without replacement. PAM clustering was independently refitted within each subsample using the same distance specification and weighting scheme. Agreement with the corresponding original phenotype assignments was assessed using the adjusted Rand index (ARI), overall assignment agreement, and phenotype-specific Jaccard indices. These analyses quantified the internal stability of the phenotype assignments.

Internal temporal validation was performed by dividing the cohort into an earlier derivation period (2009–2020) and a subsequent validation period (2021–2024). The temporal split was defined independently of recurrence outcomes. Variable transformations, domain weights, continuous-variable scaling parameters, and phenotype medoids were determined in the derivation cohort and fixed before application to the validation cohort. Each validation patient was assigned to the nearest derivation-defined medoid using the frozen distance specification, without refitting the clustering solution.

To assess temporal reproducibility independently of the frozen assignments, a separate k = 2 PAM clustering solution was derived using the validation cohort alone, without incorporating derivation-cohort medoids, frozen phenotype assignments, predefined cluster labels, or recurrence outcomes. Cluster labels were aligned to account for arbitrary label permutations before comparing the two assignment procedures. Agreement between frozen assignments and independently derived clusters was quantified using the ARI, overall assignment agreement, and phenotype-specific Jaccard indices. A complete cross-classification matrix was examined to identify discordant assignments. Associations between frozen phenotype assignments and recurrence outcomes were subsequently evaluated using the same outcome definitions and Model 4 adjustment framework as in the primary analyses. Further details are provided in Supplementary Method 3.

2.6 Statistical analysis

Continuous variables are presented as mean ± standard deviation (SD) or median [interquartile range (IQR)], as appropriate, and categorical variables as number (percentage). Between-phenotype comparisons were performed using Welch's *t* test or the Wilcoxon rank-sum test for continuous variables and Pearson's chi-square test or Fisher's exact test for categorical variables, as appropriate. No imputation was performed, and analyses were restricted to patients with complete data for the variables required in each analysis.

Cox proportional hazards models were used to examine associations between substrate phenotype and recurrence outcomes, with the lower systemic-burden phenotype serving as the reference. Separate models were fitted for early recurrence, post-blanking recurrence by 12 months after ablation, and follow-up post-blanking recurrence. Early recurrence was assessed in the full cohort, whereas post-blanking outcomes were evaluated in the 3-month landmark cohort.

Four sequential Cox models were constructed to assess the robustness of phenotype–recurrence associations across progressively adjusted models. Model 1 was unadjusted. Model 2 adjusted for sex, AF type, and ablation calendar period. Model 3 additionally adjusted for smoking status and alcohol consumption. Model 4 further adjusted for pre-ablation use of statins, β-blockers, ACEIs or ARBs, ARNIs, VKAs, NOACs, amiodarone, and dronedarone. Given the small number of patients undergoing PFA, ablation modality was excluded from the primary adjustment models and examined in a sensitivity analysis restricted to thermal ablation modalities. The 17 variables used to derive the phenotypes were not simultaneously included in the primary Cox models because they constituted the phenotype exposure. Accordingly, the resulting hazard ratios (HRs) were interpreted as associations with composite phenotypic profiles rather than effects independent of their constituent characteristics. The incremental prognostic value of phenotype membership beyond established clinical predictors was evaluated separately. HRs are reported with 95% confidence intervals (CIs).

Kaplan–Meier curves were used to estimate recurrence-free survival after the 3-month landmark, and between-phenotype differences were assessed using the log-rank test. Restricted mean survival time (RMST) was estimated at 36, 60, 90, and 120 months after the landmark. RMST differences were calculated as the higher cardiometabolic-inflammatory phenotype minus the lower systemic-burden phenotype, with negative values indicating shorter recurrence-free survival in the higher cardiometabolic-inflammatory phenotype. Percentile bootstrap 95% CIs were estimated using 500 resamples.

To investigate whether binary phenotype membership represented a simplified partition of continuous substrate heterogeneity, an outcome-independent substrate-position score was calculated from each patient's domain-balanced Gower distances to the two phenotype medoids: $S_i = \frac{d_{(x_i, m_L)}}{d_{(x_i, m_L)} + d_{(x_i, m_H)}}$, where x_i represents the pre-ablation profile of patient i, m_L and m_H denote the medoids of the lower systemic-burden and higher cardiometabolic-inflammatory phenotypes, respectively, and $d_{(\cdot,\cdot)}$ represents the domain-balanced Gower distance. Higher scores indicated greater proximity to the higher cardiometabolic-inflammatory phenotype medoid. The score was standardized and evaluated per 1-SD increment and using restricted cubic splines with four knots placed at the 5th, 35th, 65th, and 95th percentiles. Model fit and discrimination were compared using the Akaike information criterion (AIC) and Harrell's C-index, respectively.

Subgroup analyses of follow-up post-blanking recurrence were performed according to AF type, sex, age (< 65 vs ≥ 65 years), diabetes mellitus, and LAD (< 45 vs ≥ 45 mm). Subgroup-specific HRs were estimated using the Model 4 adjustment framework, with the subgroup-defining variable excluded from the adjustment set where applicable. Effect modification was assessed using phenotype-by-subgroup interaction terms. Sample sizes and event counts were reported for each subgroup stratum.

Sensitivity analyses were performed to evaluate the robustness of the association between substrate phenotype and follow-up post-blanking recurrence, using Model 4 as the reference. To assess the influence of follow-up duration, administrative censoring was applied at 24 months after the index ablation, retaining all eligible patients in the 3-month landmark cohort irrespective of recurrence status. Patients with shorter available follow-up were censored at their last documented follow-up. To examine potential secular changes in ablation practice and clinical management, calendar periods were categorized as 2009–2017, 2018–2020, and 2021–2024. Using the primary full-cohort k = 2 phenotype assignments, phenotype-by-calendar-period interactions and period-specific Cox models were evaluated. An additional analysis was restricted to patients undergoing thermal ablation (RFA or CBA), with ablation modality included as an adjustment variable. To assess the contribution of established clinical predictors included in phenotype derivation, an exploratory model additionally adjusted for age, LAD, hypertension, and diabetes mellitus. An alternative k = 3 clustering solution was evaluated to assess the influence of cluster number on phenotype–recurrence associations. Phenotypes were also re-derived after excluding age from the clustering variables to investigate the contribution of age to phenotype assignment and recurrence associations. Finally, an exploratory competing-risk analysis was performed for follow-up post-blanking recurrence, treating all-cause death before documented recurrence as a competing event. Adjusted subdistribution HRs were estimated using Fine–Gray regression with the Model 4 covariate set.

To evaluate incremental prognostic performance beyond established clinical predictors, a clinical benchmark Cox model was constructed using age, sex, AF type, BMI, LAD, LVEF, hypertension, diabetes mellitus, heart failure, and ablation calendar period. Binary phenotype membership and the continuous substrate-position score were added separately to the benchmark model. Apparent prognostic performance was evaluated using the time-dependent area under the receiver operating characteristic curve (AUC), the

Brier score estimated using inverse probability of censoring weighting (IPCW), and calibration plots. The prediction horizon was 9 months after the 3-month landmark, corresponding to 12 months after ablation. Nested models were compared using likelihood-ratio tests. Decision curve analysis was performed across recurrence-risk thresholds of 5%–35%.

Exploratory internal validation was performed using 500 out-of-bag (OOB) bootstrap resamples. In each iteration, the clinical benchmark model and both augmented Cox models were independently refitted in a bootstrap training sample and evaluated in patients not included in that sample. Incremental discrimination, prediction error, and net benefit were calculated relative to the benchmark model within the same OOB evaluation sample. Results were summarized as medians and empirical 2.5th–97.5th percentile ranges. Phenotype assignments and continuous substrate-position scores were held fixed throughout bootstrap resampling. Consequently, these analyses evaluated model performance conditional on the previously derived phenotypic representations and did not account for uncertainty arising from phenotype derivation. These OOB analyses did not validate the complete clustering and prediction pipeline. Further details are provided in Supplementary Method 4.

The proportional hazards assumption was assessed using scaled Schoenfeld residuals and corresponding covariate-specific and global tests. Where evidence of non-proportional hazards was identified, supporting Cox models incorporating appropriate stratification were fitted, and the proportional hazards assumption was reassessed. Subgroup and sensitivity analyses were considered exploratory, without adjustment for multiple comparisons. All statistical analyses were performed using R software (version 4.4.2). Two-sided *P* values < 0.05 were considered statistically significant.

2.7 Research-use phenotype assignment interface

A publicly accessible web-based research interface was developed to implement nearest-medoid phenotype assignment using routinely available pre-ablation variables. The interface displayed the assigned phenotype, distances to both medoids, and descriptive cohort-level information but did not provide individualized recurrence-risk predictions or treatment recommendations. The interface is available at https://zhangzixi237.shinyapps.io/af-phenotype-tool/. Further details are provided in Supplementary Method 5.

3. Results

3.1 Study cohort and derivation of pre-ablation substrate phenotypes

Of the 1806 adults with AF screened during the study period, 1654 met the eligibility criteria and were included in the final analytical cohort (Figure 1). Pre-ablation substrate phenotypes were derived using domain-balanced Gower distance and PAM clustering. Among the candidate solutions (k = 2–6), the k = 2 solution yielded the highest average silhouette width (0.205) (Figure 2A). This solution identified a lower systemic-burden phenotype comprising 772 patients (46.7%) and a higher cardiometabolic-inflammatory phenotype comprising 882 patients (53.3%).

PCoA showed partial separation between the two phenotypes (Figure 2B). Variable-level standardized differences and phenotype-specific substrate profiles illustrated differences in the distribution of coexisting abnormalities (Figure 2C and 2D). The largest absolute standardized differences (higher minus lower phenotype) were observed for serum albumin (−1.61), log-transformed triglycerides (1.40), age (1.40), LAD (1.33), and log-transformed CRP (1.31). At the domain level, separation was greatest for inflammatory-nutritional status (mean absolute standardized difference, 1.46), followed by atrial structural substrate (1.33), cardiometabolic substrate (0.84), renal-metabolic status (0.64), systemic comorbidity (0.55), and myocardial stress-functional status (0.47) (Figure 2E).

Repeated subsampling analyses showed relatively stable phenotype assignments. Across 500 subsamples, the mean ± SD ARI was 0.892 ± 0.071, overall assignment agreement was 0.972 ± 0.019, and phenotype-specific Jaccard indices were 0.943 ± 0.038 and 0.946 ± 0.035 for the lower systemic-burden and higher cardiometabolic-inflammatory phenotypes, respectively (Table S1).

3.2 Baseline characteristics according to substrate phenotype

Baseline characteristics according to pre-ablation substrate phenotype are summarized in Table 1. Compared with patients in the lower systemic-burden phenotype, those in the higher cardiometabolic-inflammatory phenotype were older (69.8 ± 12.4 vs 52.4 ± 12.6 years), had higher BMI (26.2 ± 3.3 vs 22.5 ± 3.3 kg/m²), and had larger LAD (46.6 ± 6.9 vs 36.9 ± 7.7 mm; all $P < 0.001$). Persistent AF was more prevalent in the higher cardiometabolic-inflammatory phenotype (31.0% vs 25.3%; $P = 0.010$), whereas LVEF was slightly lower (58.9 ± 8.2% vs 60.0 ± 7.6%; $P = 0.006$). Sex distribution did not differ significantly

between phenotypes (P = 0.310).

The higher cardiometabolic-inflammatory phenotype was characterized by greater prevalences of hypertension (61.5% vs 33.2%), diabetes mellitus (40.1% vs 28.9%), dyslipidemia (59.2% vs 11.7%), heart failure (25.1% vs 18.5%), coronary heart disease (20.1% vs 15.0%), and obstructive sleep apnea (5.1% vs 2.6%). Laboratory profiles showed higher HbA1c, triglycerides, CRP, uric acid, and NT-proBNP, together with lower serum albumin (33.9 ± 4.9 vs 41.4 ± 4.4 g/L) and eGFR (75.6 ± 17.1 vs 91.7 ± 17.8 mL/min/1.73 m²) in the higher cardiometabolic-inflammatory phenotype.

Pre-ablation use of statins, ACEIs or ARBs, and ARNIs was more frequent in the higher cardiometabolic-inflammatory phenotype, whereas β-blocker, VKA, NOAC, amiodarone, and dronedarone use did not differ significantly between groups. The distribution of ablation modalities was also comparable between phenotypes (P = 0.134). Overall, RFA accounted for 1372 procedures (83.0%), CBA for 277 (16.7%), and PFA for only 5 (0.3%).

3.3 Recurrence outcomes, sequential Cox associations, and recurrence-free survival

The median follow-up duration from the index ablation was 60 months (IQR: 36–96 months) in the overall cohort, 60 months (IQR: 48–96 months) in the lower systemic-burden phenotype, and 48 months (IQR: 36–84 months) in the higher cardiometabolic-inflammatory phenotype. Early recurrence within 3 months occurred in 102 of 1654 patients (6.2%). After exclusion of patients with documented early recurrence, 1552 patients constituted the 3-month landmark cohort. Post-blanking recurrence by 12 months after ablation was documented in 233 patients (15.0%), whereas follow-up post-blanking recurrence was documented in 408 patients (26.3%).

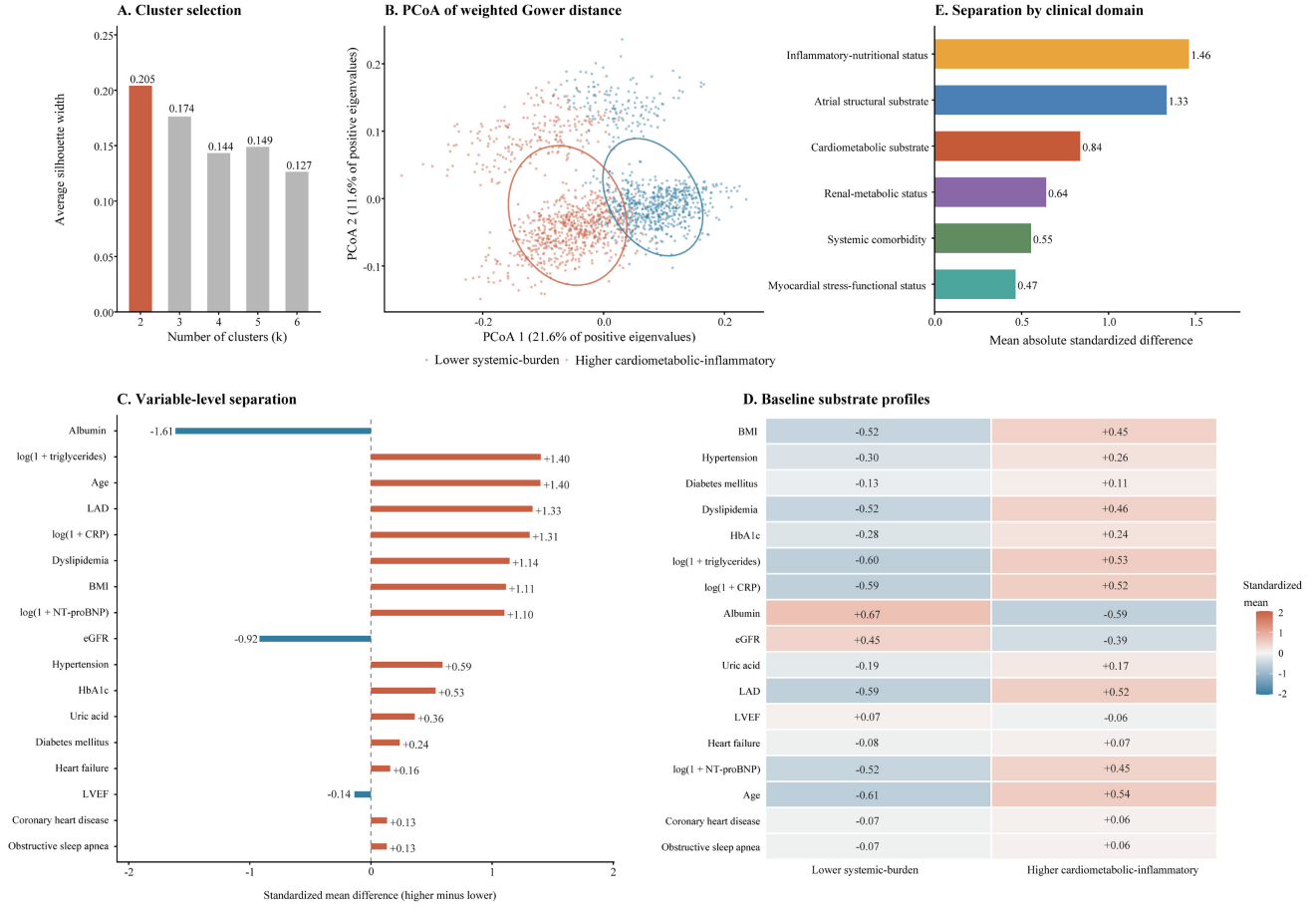


Figure 2. Derivation and characterization of pre-ablation substrate phenotypes. (A) Average silhouette width across candidate PAM clustering solutions (k = 2–6). (B) PCoA illustrating the distribution of patients assigned to the lower systemic-burden and higher cardiometabolic-inflammatory phenotypes based on domain-balanced Gower distances. (C) Variable-level separation between phenotypes, quantified using standardized mean differences (higher minus lower phenotype). (D) Heatmap showing phenotype-specific standardized mean values for the 17 pre-ablation variables used in clustering. (E) Separation across the six prespecified clinical domains, summarized by the mean absolute standardized difference of the constituent variables within each domain. Abbreviations: BMI, body mass index; CRP, C-reactive protein; eGFR, estimated glomerular filtration rate; HbA1c, glycated hemoglobin; LAD, left atrial diameter; LVEF, left ventricular ejection fraction; NT-proBNP, N-terminal pro-B-type natriuretic peptide; PAM, partitioning around medoids; PCoA, principal coordinates analysis.

Table 1. Baseline characteristics according to pre-ablation substrate phenotype.

Characteristic	Overall (N = 1654)	Lower systemic-burden phenotype (N = 772)	Higher cardiometabolic-inflammatory phenotype (N = 882)	*P* value
Age, years	61.7 ± 15.2	52.4 ± 12.6	69.8 ± 12.4	< 0.001
Sex, n (%)				0.310
Female	681 (41.2)	328 (42.5)	353 (40.0)	
Male	973 (58.8)	444 (57.5)	529 (60.0)	
Smoking status, n (%)	505 (30.5)	210 (27.2)	295 (33.4)	0.006
Alcohol consumption, n (%)	364 (22.0)	158 (20.5)	206 (23.4)	0.157
BMI, kg/m²	24.5 ± 3.8	22.5 ± 3.3	26.2 ± 3.3	< 0.001
AF type, n (%)				0.010
Paroxysmal AF	1186 (71.7)	577 (74.7)	609 (69.0)	
Persistent AF	468 (28.3)	195 (25.3)	273 (31.0)	
LAD, mm	42.1 ± 8.7	36.9 ± 7.7	46.6 ± 6.9	< 0.001
LVEF, %	59.4 ± 7.9	60.0 ± 7.6	58.9 ± 8.2	0.006
Hypertension, n (%)	798 (48.2)	256 (33.2)	542 (61.5)	< 0.001
Diabetes mellitus, n (%)	577 (34.9)	223 (28.9)	354 (40.1)	< 0.001
Dyslipidemia, n (%)	612 (37.0)	90 (11.7)	522 (59.2)	< 0.001
Heart failure, n (%)	364 (22.0)	143 (18.5)	221 (25.1)	0.001
Coronary heart disease, n (%)	293 (17.7)	116 (15.0)	177 (20.1)	0.007
Obstructive sleep apnea, n (%)	65 (3.9)	20 (2.6)	45 (5.1)	0.009
NT-proBNP, pg/mL	220.7 (110.1–417.4)	114.5 (60.3–215.1)	400.0 (217.5–451.5)	< 0.001
HbA1c, %	6.4 ± 0.9	6.1 ± 0.9	6.6 ± 0.9	< 0.001
Triglycerides, mmol/L	1.3 (0.9–1.9)	1.0 (0.8–1.2)	1.8 (1.4–2.5)	< 0.001
CRP, mg/L	6.3 (1.4–7.3)	1.5 (0.5–4.1)	7.2 (6.3–7.8)	< 0.001
Albumin, g/L	37.4 ± 6.0	41.4 ± 4.4	33.9 ± 4.9	< 0.001
eGFR, mL/min/1.73 m²	83.1 ± 19.2	91.7 ± 17.8	75.6 ± 17.1	< 0.001
Uric acid, μmol/L	359.2 ± 98.9	340.5 ± 95.2	375.6 ± 99.2	< 0.001
Statin use, n (%)	715 (43.2)	271 (35.1)	444 (50.3)	< 0.001
β-blocker use, n (%)	813 (49.2)	367 (47.5)	446 (50.6)	0.219
ACEI/ARB use, n (%)	579 (35.0)	247 (32.0)	332 (37.6)	0.016
ARNI use, n (%)	145 (8.8)	47 (6.1)	98 (11.1)	< 0.001
VKA use, n (%)	586 (35.4)	287 (37.2)	299 (33.9)	0.165
NOAC use, n (%)	924 (55.9)	415 (53.8)	509 (57.7)	0.106
Amiodarone use, n (%)	1056 (63.8)	502 (65.0)	554 (62.8)	0.350
Dronedarone use, n (%)	189 (11.4)	80 (10.4)	109 (12.4)	0.203
Ablation modality, n (%)				0.134
RFA	1372 (83.0)	628 (81.3)	744 (84.4)	
CBA	277 (16.7)	140 (18.1)	137 (15.5)	
PFA	5 (0.3)	4 (0.5)	1 (0.1)	

Continuous variables are presented as mean ± SD or median (IQR), as appropriate, and categorical variables as number (percentage).

Abbreviations: ACEI, angiotensin-converting enzyme inhibitor; AF, atrial fibrillation; ARB, angiotensin receptor blocker; ARNI, angiotensin receptor–neprilysin inhibitor; BMI, body mass index; CBA, cryoballoon ablation; CRP, C-reactive protein; eGFR, estimated glomerular filtration rate; HbA1c, glycated hemoglobin; IQR, interquartile range; LAD, left atrial diameter; LVEF, left ventricular ejection fraction; NOAC, non-vitamin K antagonist oral anticoagulant; NT-proBNP, N-terminal pro-B-type natriuretic peptide; PFA, pulsed field ablation; RFA, radiofrequency ablation; SD, standard deviation; VKA, vitamin K antagonist.

The observed proportion of early recurrence was 5.4% (42/772) in the lower systemic-burden phenotype and 6.8% (60/882) in the higher cardiometabolic-inflammatory phenotype, with no statistically significant between-phenotype difference (P = 0.251) (Figure 3). In contrast, post-blanking recurrence by 12 months was more frequent in the higher cardiometabolic-inflammatory phenotype than in the lower systemic-burden phenotype [22.0% (181/822) vs 7.1% (52/730); P < 0.001]. A similar difference was observed for follow-up post-blanking recurrence [36.0% (296/822) vs 15.3% (112/730); P < 0.001].

Sequential Cox regression models showed consistent associations between the higher cardiometabolic-inflammatory phenotype and post-blanking recurrence (Table 2). In Model 4, the higher cardiometabolic-inflammatory phenotype was not significantly associated with early recurrence (HR: 1.19, 95% CI: 0.80–1.79; P = 0.388). In contrast, it was associated with post-blanking recurrence by 12 months (HR: 3.47, 95% CI: 2.54–4.75; P < 0.001) and follow-up post-blanking recurrence (HR: 2.85, 95% CI: 2.28–3.56; P < 0.001).

Table 2. Associations between pre-ablation substrate phenotype and recurrence outcomes across sequential Cox regression models.

Outcome	Events/Number	Model 1	Model 2	Model 3	Model 4
		HR (95% CI) *P* value	HR (95% CI) *P* value	HR (95% CI) *P* value	HR (95% CI) *P* value
Early recurrence within 3 months	102/1654	1.25 (0.85–1.86) 0.261	1.22 (0.82–1.82) 0.316	1.23 (0.82–1.82) 0.314	1.19 (0.80–1.79) 0.388
Post-blanking recurrence by 12 months	233/1552	3.35 (2.46–4.56) < 0.001	3.41 (2.50–4.65) < 0.001	3.41 (2.50–4.65) < 0.001	3.47 (2.54–4.75) < 0.001
Follow-up post-blanking recurrence	408/1552	2.83 (2.28–3.52) < 0.001	2.89 (2.32–3.59) < 0.001	2.89 (2.32–3.60) < 0.001	2.85 (2.28–3.56) < 0.001

HRs and 95% CIs compare the higher cardiometabolic-inflammatory phenotype with the lower systemic-burden phenotype (reference). Model 1 was unadjusted. Model 2 adjusted for sex, AF type, and ablation calendar period. Model 3 additionally adjusted for smoking status and alcohol consumption. Model 4 further adjusted for pre-ablation use of statins, β-blockers, ACEIs or ARBs, ARNIs, VKAs, NOACs, amiodarone, and dronedarone. Early recurrence was evaluated in the full cohort, whereas post-blanking outcomes were evaluated in the 3-month landmark cohort.

Abbreviations: ACEI, angiotensin-converting enzyme inhibitor; AF, atrial fibrillation; ARB, angiotensin receptor blocker; ARNI, angiotensin receptor–neprilysin inhibitor; CI, confidence interval; HR, hazard ratio; NOAC, non-vitamin K antagonist oral anticoagulant; VKA, vitamin K antagonist.

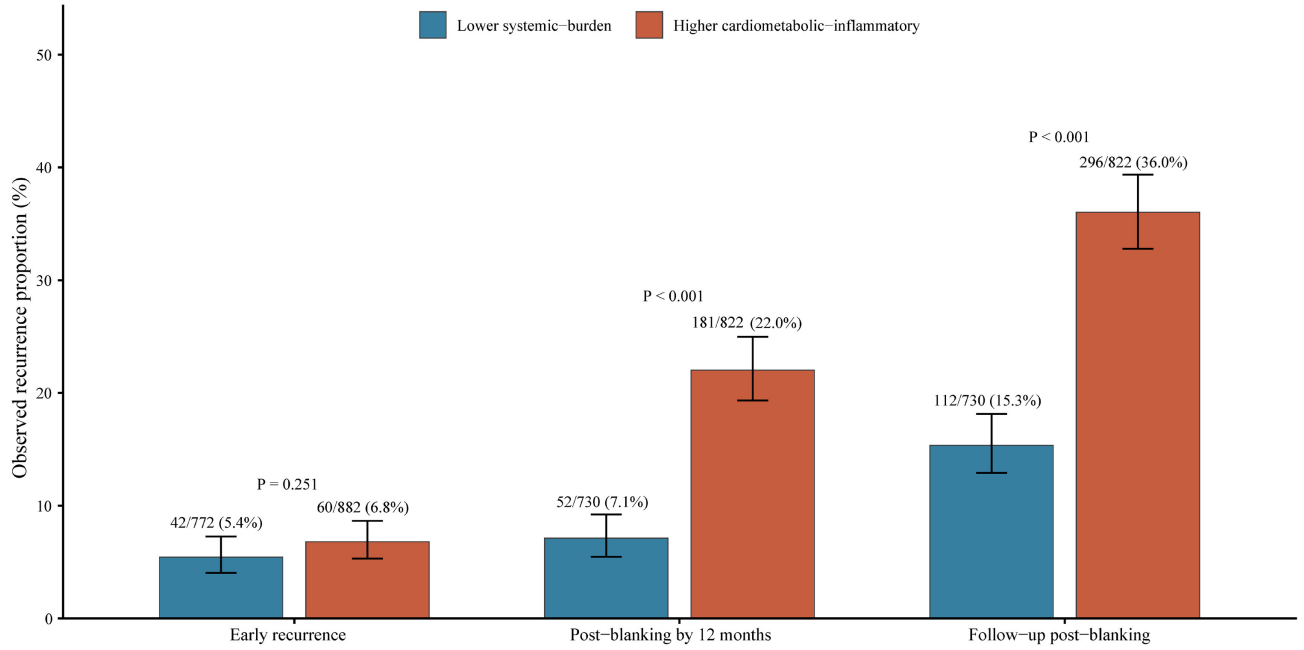


Figure 3. Observed recurrence proportions according to pre-ablation substrate phenotype. Observed proportions of early recurrence within 3 months, post-blanking recurrence by 12 months after ablation, and follow-up post-blanking recurrence are shown for the lower systemic-burden and higher cardiometabolic-inflammatory phenotypes. Early recurrence was evaluated in the full cohort, whereas post-blanking outcomes were evaluated in the 3-month landmark cohort. Values are presented as events/number of patients (percentage), with error bars indicating 95% CIs. *P* values represent between-phenotype comparisons of observed recurrence proportions. Abbreviations: CI, confidence interval.

Kaplan–Meier analysis showed lower recurrence-free survival in the higher cardiometabolic-inflammatory phenotype after the 3-month landmark (log-rank $P < 0.001$) (Figure 4). RMST analyses demonstrated progressively larger absolute differences in recurrence-free survival over longer time horizons (Figure S1). The RMST differences (higher minus lower phenotype) were −5.58 months (95% bootstrap CI: −6.67 to −4.43) at 36 months, −11.09 months (95% bootstrap CI: −13.19 to −8.95) at 60 months, −17.96 months (95% bootstrap CI: −21.61 to −14.58) at 90 months, and −24.78 months (95% bootstrap CI: −29.90 to −19.94) at 120 months after the landmark.

Schoenfeld residual analyses showed no evidence of non-proportional hazards for the phenotype term in any of the three primary Cox models (Table S2). However, the global proportional hazards test was significant for the primary model of post-blanking recurrence by 12 months ($P = 0.013$), with covariate-specific evidence of non-proportionality for β-blocker and dronedarone use. In a supporting Cox model stratified by these medication variables, the phenotype association remained similar to that in the primary model (HR: 3.49, 95% CI: 2.55–4.77; $P < 0.001$), and the global proportional hazards test was no longer statistically significant ($P = 0.153$).

3.4 Subgroup and sensitivity analyses for follow-up post-blanking recurrence

Subgroup analyses showed directionally consistent associations between the higher cardiometabolic-inflammatory phenotype and follow-up post-blanking recurrence across strata defined by AF type, sex, age, diabetes mellitus, and LAD (Figure 5). Subgroup-specific adjusted HRs ranged from 2.11 to 3.48. Although the association was numerically stronger among patients aged ≥ 65 years than among

younger patients, the phenotype-by-age interaction was not statistically significant (P for interaction = 0.066). No statistically significant interactions were detected for AF type (P = 0.638), sex (P = 0.280), diabetes mellitus (P = 0.434), or LAD (P = 0.456).

Sensitivity analyses yielded estimates consistent with the primary phenotype–recurrence association (Figure S2). With uniform administrative censoring at 24 months after ablation, the higher cardiometabolic-inflammatory phenotype remained associated with follow-up post-blanking recurrence (319 events; HR: 2.89, 95% CI: 2.24–3.73; P < 0.001). Similar results were obtained after restricting the analysis to patients undergoing thermal ablation (RFA or CBA; n = 1547, 407 events; HR: 2.86, 95% CI: 2.29–3.57; P < 0.001). Additional adjustment for age, LAD, hypertension, and diabetes mellitus attenuated the association, although it remained statistically significant (HR: 2.07, 95% CI: 1.53–2.80; P < 0.001).

Calendar-period analyses yielded directionally consistent estimates across 2009–2017 (HR: 3.39, 95% CI: 2.20–5.20), 2018–2020 (HR: 2.80, 95% CI: 1.80–4.35), and 2021–2024 (HR: 2.70, 95% CI: 2.01–3.62). There was no statistically significant phenotype-by-calendar-period interaction (P = 0.490) (Table S3).

An alternative k = 3 clustering solution identified lower, intermediate, and higher substrate-burden phenotypes (Tables S4–S6). Compared with the lower substrate-burden phenotype in this alternative solution, the intermediate substrate-burden phenotype (adjusted HR: 1.59, 95% CI: 1.18–2.15) and the higher substrate-burden phenotype (adjusted HR: 2.65, 95% CI: 2.02–3.47) were associated with follow-up post-blanking recurrence, with a stronger association observed for the higher substrate-burden phenotype. In a separate exploratory analysis, excluding age from phenotype derivation substantially altered phenotype assignments (ARI relative to the primary partition: 0.171; overall agreement: 70.7%). Nevertheless, the higher substrate-burden phenotype derived without age remained associated with follow-up post-blanking recurrence (HR: 2.71, 95% CI: 2.19–3.35), with attenuation after additional adjustment for age (HR: 2.06, 95% CI: 1.61–2.64) (Table S7).

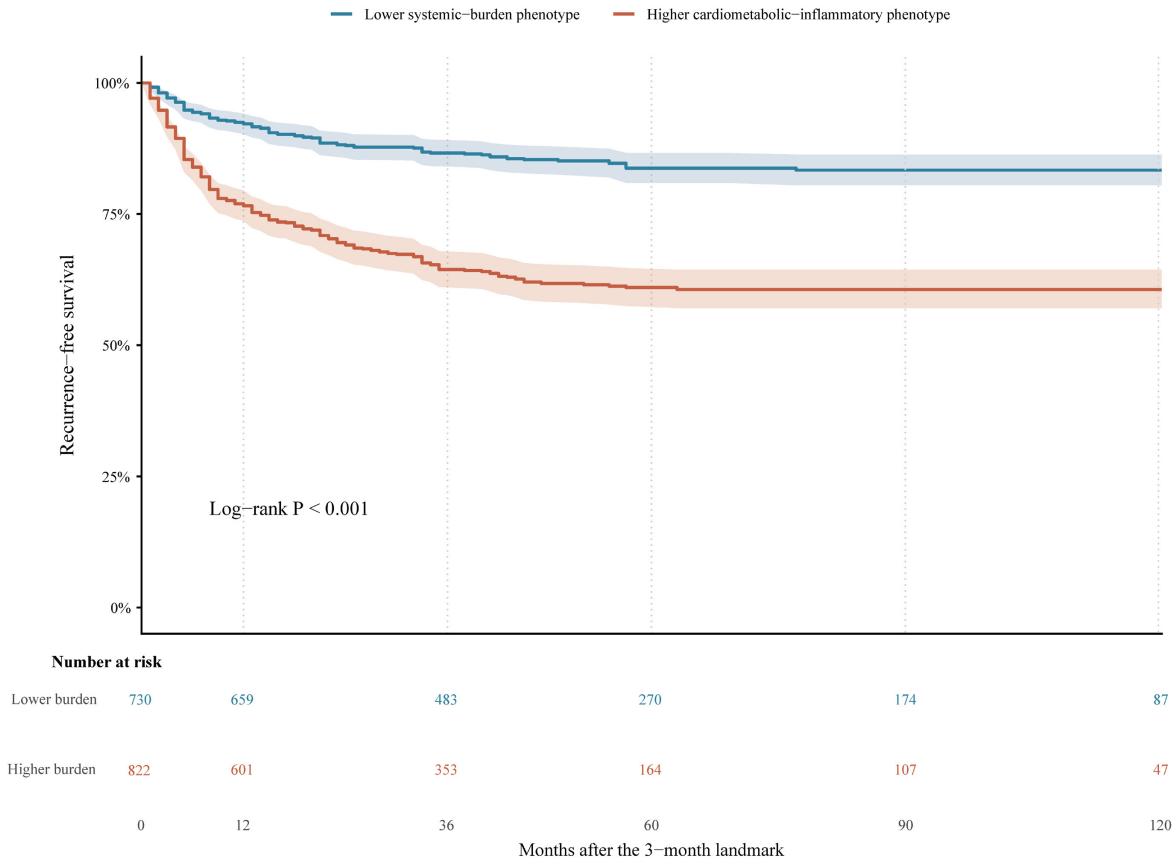


Figure 4. Kaplan–Meier estimates of recurrence-free survival after the 3-month landmark according to pre-ablation substrate phenotype. Shaded areas indicate 95% CIs, and the table below the curves shows the number of patients at risk at each indicated time point. Follow-up time was calculated from the 3-month landmark. Abbreviations: CI, confidence interval.

In an exploratory competing-risk analysis that treated all-cause death before documented AF recurrence as a competing event, 15 competing deaths were identified. The higher cardiometabolic-inflammatory phenotype remained associated with follow-up post-blanking recurrence (subdistribution HR: 2.68, 95% CI: 2.16–3.32; $P < 0.001$) (Table S8).

3.5 Internal temporal validation and continuous representation of substrate heterogeneity

Internal temporal validation was conducted using an earlier derivation cohort of 631 patients treated during 2009–2020 and a subsequent validation cohort of 1023 patients treated during 2021–2024. Application of the frozen derivation-defined phenotyping framework assigned 398 validation patients to the lower systemic-burden phenotype and 625 to the higher cardiometabolic-inflammatory phenotype. Comparison with independently performed de novo clustering in the validation cohort showed substantial, although incomplete, agreement in phenotype assignments (Figure S3A and Table S9). The ARI was 0.775, with an overall assignment agreement of 94.0% (962/1023). Phenotype-specific Jaccard indices were 0.866 for the lower systemic-burden phenotype and 0.903 for the higher cardiometabolic-inflammatory phenotype, with 61 patients (6.0%) receiving discordant assignments. Average silhouette widths were 0.201 for the frozen assignments and 0.207 for the independently derived validation clusters.

Within the temporal-validation cohort, the higher cardiometabolic-inflammatory phenotype identified using the frozen assignment framework was associated with post-blanking recurrence by 12 months (HR: 3.74, 95% CI: 2.36–5.91; $P < 0.001$) and follow-up post-blanking recurrence (HR: 2.79, 95% CI: 2.04–3.82; $P < 0.001$). In contrast, the association with early recurrence was not statistically significant (HR: 1.29, 95% CI: 0.78–2.12; $P = 0.318$) (Figure S3B and Table S9).

The continuous substrate-position score provided an alternative representation of multidomain substrate heterogeneity. In the linear Cox model, each 1-SD increase in the score was associated with a higher hazard of follow-up post-blanking recurrence (HR: 1.80, 95% CI: 1.61–2.01; $P < 0.001$). Restricted cubic spline analysis demonstrated a significant overall association and evidence of nonlinearity (both $P < 0.001$) (Figure S4). Relative to the Cox model containing only the Model 4 covariates, adding binary phenotype membership reduced the AIC from 5811.2 to 5719.5 and increased Harrell's C-index from 0.561 to 0.652. Adding the continuous substrate-position score yielded an AIC of 5727.4 and a C-index of 0.655 (Table S10).

3.6 Incremental prognostic and decision-analytic performance

Incremental prognostic performance was evaluated in the 3-month landmark cohort of 1552 patients, including 233 with documented post-blanking recurrence by 12 months after ablation. At the prespecified prediction horizon of 9 months after the landmark, the clinical benchmark model achieved an apparent time-dependent AUC of 0.6941. Adding binary phenotype membership increased the AUC to 0.7068 (ΔAUC: +0.0127), whereas adding the continuous substrate-position score increased it to 0.7063 (ΔAUC: +0.0122). Both augmented models showed improved apparent model fit according to likelihood-ratio testing (both $P < 0.001$). Corresponding IPCW Brier scores were 0.1204 for the clinical benchmark model, 0.1189 for the binary phenotype model, and 0.1195 for the continuous score model, indicating modest reductions in prediction error (Table S11).

Across 500 OOB bootstrap evaluations, the median ΔAUC was +0.0155 (empirical 2.5th–97.5th percentile range: −0.0162 to +0.0330) for binary phenotype membership and +0.0138 (−0.0123 to +0.0269) for the continuous score. Although the median estimates favored both augmented models, the empirical percentile ranges included negative values, indicating variability in incremental discrimination across OOB evaluations. Reductions in Brier scores were similarly modest and variable (Table S11).

Apparent calibration was similar across the three models (Figure S5). Decision curve analysis showed small differences in net benefit across the evaluated recurrence-risk thresholds (Figure S6). At a 15% risk threshold, apparent net benefit increased from 0.0428 for the clinical benchmark model to 0.0507 with binary phenotype membership and 0.0477 with the continuous score. The corresponding median OOB incremental net benefits were +0.00711 (empirical 2.5th–97.5th percentile range: −0.00420 to +0.01965) and +0.00524 (−0.00424 to +0.01744), respectively.

3.7 Research-use phenotype assignment interface

The publicly accessible research-use interface demonstrated nearest-medoid phenotype assignment using the prespecified pre-ablation variables. The interface displayed the assigned phenotype, distances to the two phenotype medoids, and descriptive cohort-level information (Figure S7).

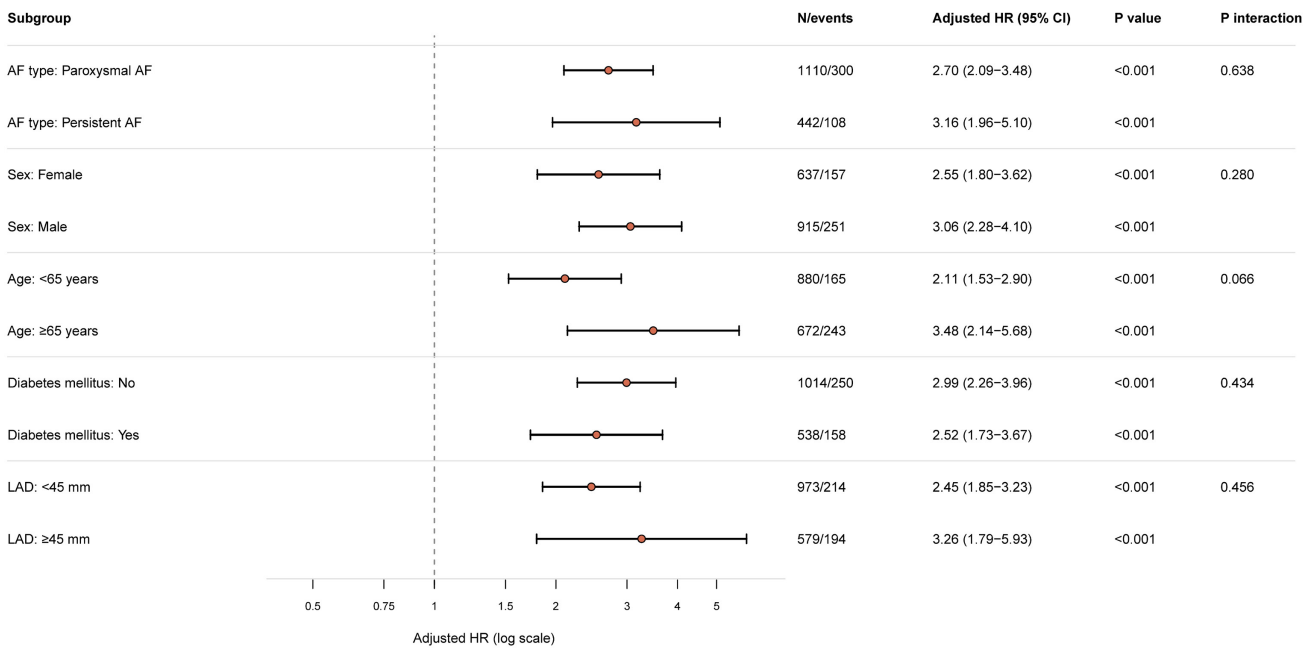


Figure 5. Subgroup associations between pre-ablation substrate phenotype and follow-up post-blanking recurrence. Adjusted HRs and 95% CIs compare the higher cardiometabolic-inflammatory phenotype with the lower systemic-burden phenotype across subgroups defined by AF type, sex, age, diabetes mellitus, and LAD. Subgroup-specific Cox models followed the Model 4 adjustment framework, excluding the subgroup-defining variable when applicable. Interaction *P* values were derived from phenotype-by-subgroup interaction tests. The numbers of patients and recurrence events are presented for each subgroup stratum. Abbreviations: AF, atrial fibrillation; CI, confidence interval; HR, hazard ratio; LAD, left atrial diameter.

4. Discussion

In patients undergoing first-time catheter ablation for AF, outcome-independent analysis of 17 pre-ablation variables identified two clinically interpretable patterns of multidomain substrate burden. The higher cardiometabolic-inflammatory phenotype was associated with substantially greater recurrence after the blanking period, whereas the association with early recurrence was not statistically significant. The phenotypic structure remained reasonably consistent across subsampling and temporal analyses, and a continuous substrate-position score demonstrated a nonlinear relationship with recurrence.

The durability of rhythm control after pulmonary vein isolation depends not only on eliminating initiating triggers but also on the atrial environment in which recurrent arrhythmias may be sustained [6, 8]. Atrial enlargement reflects one dimension of this environment, whereas obesity, diabetes, hypertension, impaired renal function, and altered inflammatory and myocardial stress markers capture partly overlapping systemic processes. Metabolic dysregulation and hemodynamic loading have been implicated in atrial stretch, extracellular matrix remodeling, and conduction heterogeneity; inflammation and neurohormonal activation may further reinforce electrical and structural abnormalities [5, 6, 19]. AF may also aggravate hemodynamic and neurohormonal disturbances, making the relationship between arrhythmia and substrate bidirectional [19]. In the higher cardiometabolic-inflammatory phenotype, larger atrial diameter coincided with greater adiposity, cardiometabolic comorbidity, elevated CRP and NT-proBNP, and lower albumin and eGFR.

Associations between phenotype membership and recurrence differed between the early and post-blanking periods. Early atrial tachyarrhythmias occur while tissue injury, autonomic responses, lesion maturation, and transient conduction changes may influence rhythm independently of baseline substrate burden [8, 20]. Transient postprocedural mechanisms may partly explain the weaker association with early recurrence. Beyond the blanking period, the higher cardiometabolic-inflammatory phenotype was associated with both 12-month recurrence and recurrence over subsequent follow-up, accompanied by progressively greater differences in restricted mean recurrence-free survival. The stronger association with post-blanking recurrence suggests that baseline substrate burden may be more closely related to later recurrence than to early postprocedural arrhythmias. Accordingly, the post-blanking estimates apply to patients who remained under follow-up without documented recurrence at the 3-month landmark.

Outcome-independent clustering characterized patterns of coexisting pre-ablation abnormalities

without using recurrence outcomes to define patient groups. Previous unsupervised clustering research similarly identified clinical phenotypes associated with recurrence after AF ablation [16]. Equal weighting across the six clinical domains limited the influence of differences in the number of variables assigned to each domain. Modest cluster separation, together with the nonlinear association between the continuous substrate-position score and recurrence, suggested that the identified phenotypes represented different regions of a continuous multidimensional substrate distribution. The graded associations observed in the exploratory three-cluster analysis were also consistent with a continuous distribution of substrate burden. Binary phenotypes summarize this spectrum efficiently, whereas a continuous representation retains information about relative proximity to the two phenotypic centers.

Assignment stability was favorable under repeated subsampling, and phenotype assignments based on the frozen derivation-defined framework showed 94.0% agreement with independently derived clusters in patients treated during a later era. An ARI of 0.775 suggested persistence of the dominant patterns across treatment periods. The agreement estimates were based on comparisons between frozen derivation-defined assignments and clusters independently derived in the temporal-validation cohort. At the same time, the substantial redistribution of patients after excluding age illustrates the contribution of demographic context to the phenotype boundaries. The sensitivity of phenotype assignments to age is consistent with the association of aging with atrial remodeling and the accumulation of cardiometabolic comorbidities [4, 19].

Adjustment for age, LAD, hypertension, and diabetes reduced the association with follow-up recurrence from an HR of 2.85 to 2.07. This attenuation indicates that established clinical determinants contributed to the observed phenotype–recurrence association, while the remaining association suggests that the broader phenotypic profiles captured additional variation beyond these four characteristics. The reported associations therefore reflect composite clinical phenotypes rather than effects independent of their constituent characteristics. Associations remained broadly consistent across calendar periods and after administrative censoring, restriction to thermal ablation, and accounting for competing death.

Incremental prognostic performance was modest despite the observed associations between phenotype membership and recurrence. When added to a clinical benchmark model, binary phenotype membership increased apparent time-dependent discrimination from 0.6941 to 0.7068, with a comparable increase for the continuous score. Changes in prediction error and decision-curve net benefit were likewise small, and OOB estimates varied across resampled evaluations. The phenotypes summarized patterns of coexisting clinical abnormalities but provided only modest additional prognostic information beyond the benchmark model. Several phenotype-defining characteristics were already included in the clinical benchmark model, which may partly explain the limited improvement in discrimination.

Evidence that comprehensive risk-factor management can improve rhythm outcomes after AF ablation supports further investigation of whether multidomain profiles correspond to different trajectories of AF progression or responses to upstream risk-factor modification [21]. Integration with atrial imaging, electroanatomic substrate mapping, longitudinal biomarkers, and standardized rhythm monitoring could clarify which phenotype features most closely track tissue remodeling and post-ablation recurrence. External validation and prospective studies are needed to determine whether these phenotypes provide additional information relevant to recurrence surveillance or treatment selection.

5. Limitations

Several limitations warrant consideration. First, the single-center retrospective design may have introduced selection bias and residual confounding. Analyses were restricted to patients with the required clinical and follow-up information, which may affect generalizability. Subsampling and internal temporal analyses supported the reproducibility of phenotype assignments, but independent external validation remains necessary. Second, recurrence was ascertained through routine clinical follow-up rather than systematic continuous rhythm monitoring. Asymptomatic or brief atrial tachyarrhythmias may therefore have been missed. Patients with greater cardiometabolic comorbidity may have had more frequent healthcare encounters and opportunities for opportunistic electrocardiographic assessment, potentially increasing recurrence detection in the higher cardiometabolic-inflammatory phenotype and exaggerating the observed association with recurrence. Because detailed patient-level information on rhythm-monitoring intensity was not consistently available, we could not quantify or adequately adjust for differential surveillance. Standardized rhythm surveillance in future studies would allow a more reliable assessment of phenotype-associated recurrence. Third, the study spanned 2009–2024, during which ablation technologies, procedural management, and follow-up practices evolved.

Calendar-period and thermal ablation-restricted analyses yielded consistent associations, although residual effects of changing clinical practice remain possible. The small number of patients undergoing PFA also precluded meaningful modality-specific evaluation. Fourth, post-blanking analyses were based on a 3-month landmark cohort excluding patients with documented early recurrence. The resulting associations therefore apply to patients who remained under follow-up without documented recurrence at that landmark. The 3-month blanking period was retained for consistency with the historical study framework, whereas the 2024 international expert consensus recommended an 8-week blanking period [8, 18]. This difference should be considered when comparing findings across studies. Fifth, phenotyping relied on routinely available clinical, laboratory, and echocardiographic variables without direct assessment of atrial fibrosis, electroanatomic substrate characteristics, epicardial adipose tissue, or longitudinal changes in risk-factor control. The modest cluster separation and sensitivity of phenotype assignments to variable selection indicate that the identified profiles represent simplified descriptions of multidomain substrate heterogeneity. The primary Cox models evaluated composite phenotype associations, and the additional constituent-variable adjustment did not establish independence from all phenotype-defining characteristics. Finally, incremental improvements in discrimination and decision-curve net benefit were modest. The OOB bootstrap analyses held phenotype assignments and substrate-position scores fixed and therefore evaluated prognostic performance conditional on the derived representations rather than the complete phenotyping pipeline. The research-use interface illustrates phenotype assignment but has not undergone independent validation for clinical prediction or decision-making.

6. Conclusion

In patients undergoing first-time AF catheter ablation, outcome-independent multidomain phenotyping identified two pre-ablation clinical profiles associated with different rates of post-blanking recurrence. Phenotype assignments showed internal stability and temporal reproducibility, whereas incremental prognostic performance beyond established clinical predictors was modest. External validation is needed to determine the generalizability and clinical utility of these phenotypes.

Abbreviations

ACEI: angiotensin-converting enzyme inhibitor
AF: atrial fibrillation
AIC: Akaike information criterion
ARB: angiotensin receptor blocker
ARI: adjusted Rand index
ARNI: angiotensin receptor–neprilysin inhibitor
AUC: area under the receiver operating characteristic curve
BMI: body mass index
CBA: cryoballoon ablation
CI: confidence interval
CRP: C-reactive protein
eGFR: estimated glomerular filtration rate
HbA1c: glycated hemoglobin
HR: hazard ratio
IPCW: inverse probability of censoring weighting
IQR: interquartile range
LAD: left atrial diameter
LVEF: left ventricular ejection fraction
NOAC: non-vitamin K antagonist oral anticoagulant
NT-proBNP: N-terminal pro-B-type natriuretic peptide
OOB: out-of-bag
PAM: partitioning around medoids
PCoA: principal coordinates analysis
PFA: pulsed field ablation
RFA: radiofrequency ablation
RMST: restricted mean survival time
SD: standard deviation
VKA: vitamin K antagonist

Supplementary Material

Supplementary methods and tables.
https://www.medsci.org/v23p3806s1.pdf

Acknowledgments

The graphical abstract was created in BioRender. Dai, Y. (2026) https://BioRender.com/zwu8042 (agreement number: KR2AEQQVG1).

Funding

This work was supported by the National Natural Science Foundation of China (nos. 82070356 and 81770337); the Scientific Research Program of FuRong Laboratory (no. 2025PT5001); the Chinese Society of Cardiology Foundation (no. CSCF2024B02); the Young Backbone Talent Project of Health High-Level Talents under the Furong Plan of Hunan Province (no. 20241226079); the Hunan Provincial Young Backbone Teacher Project for Ordinary Universities (no. 206030802); the Natural Science Foundation of Hunan Province (nos. 2021JJ30033 and 2024JJ9198); the Key Project of Hunan Provincial Science and Technology Innovation (no. 2024JK2119); and the Clinical Medical Technology Innovation

Guidance Project of the Hunan Provincial Science and Technology Agency (no. 2021SK53519).

Data availability

The data supporting the findings of this study are available from the corresponding author upon reasonable request. The research-use phenotype assignment interface is publicly accessible at https://zhangzixi237.shinyapps.io/af-phenotype-tool/.

Author contributions

Xunhua Wang, Xiaoyu Zeng, Jiaxin Chi, Haoqing Yu, and Ke Hu collected the study data. Siyuan Tan and Kangrong Li performed the statistical analyses. Tao Tu, Yichao Xiao, Qiming Liu, and Qiuzhen Lin prepared the data visualizations. Zixi Zhang drafted the manuscript, which was critically revised by Yongguo Dai and Chan Liu. All authors contributed to the interpretation of the findings, reviewed the manuscript, and approved the final version.

Ethics approval

This retrospective study was approved by the Biomedical Research Ethics Committee of The Second Xiangya Hospital, Central South University (approval No. LYEC2026-0047). The study was conducted in accordance with the Declaration of Helsinki, and the requirement for written informed consent was waived by the ethics committee because the study involved retrospective analysis of de-identified clinical data.

Competing Interests

The authors have declared that no competing interest exists.

References

1. Becher N, Metzner A, Toennis T, Kirchhof P, Schnabel RB. Atrial fibrillation burden: a new outcome predictor and therapeutic target. Eur Heart J. 2024; 45: 2824-38.
2. Tan S, Zhang Z, Lin Q, Tu T, Zhu J, Zeng G, et al. Burden and age-specific trends of atrial fibrillation/atrial flutter from 1990 to 2023: a growing challenge among younger and middle-aged adults. Europace. 2026;28(4):euag036.
3. Lane DA, Andrade JG, Arbelo E, Boriani G, Hendriks JM, Lee SR, et al. Atrial fibrillation. Lancet. 2026; 407: 1000-13.
4. Elliott AD, Middeldorp ME, Van Gelder IC, Albert CM, Sanders P. Epidemiology and modifiable risk factors for atrial fibrillation. Nat Rev Cardiol. 2023; 20: 404-17.
5. Bode D, Pronto JRD, Schiattarella GG, Voigt N. Metabolic remodelling in atrial fibrillation: manifestations, mechanisms and clinical implications. Nat Rev Cardiol. 2024; 21: 682-700.
6. McCauley MD, Iacobellis G, Li N, Nattel S, Goldberger JJ. Targeting the Substrate for Atrial Fibrillation: JACC Review Topic of the Week. J Am Coll Cardiol. 2024; 83: 2015-27.
7. Van Gelder IC, Rienstra M, Bunting KV, Casado-Arroyo R, Caso V, Crijns H, et al. 2024 ESC Guidelines for the management of atrial fibrillation developed in collaboration with the European Association for Cardio-Thoracic Surgery (EACTS). Eur Heart J. 2024; 45: 3314-414.
8. Tzeis S, Gerstenfeld EP, Kalman J, Saad EB, Shamloo AS, Andrade JG, et al. 2024 European Heart Rhythm Association/Heart Rhythm Society/Asia Pacific Heart Rhythm Society/Latin American Heart Rhythm Society expert consensus statement on catheter and surgical ablation of atrial fibrillation. Heart Rhythm. 2024; 21: e31-e149.
9. Zhang Z, Sun C, Tan S, Xiao Y, Tu T, Lin Q, et al. Neutrophil-to-lymphocyte ratio as a predictor of post-ablation recurrence in hypertensive patients with paroxysmal atrial fibrillation. Int J Med Sci. 2026; 23: 529-42.
10. Zhang Z, Li S, Tu T, Liu C, Dai Y, Wang C, et al. Nonlinear relationship and predictive value of systemic immune-inflammation index for atrial fibrillation recurrence after catheter ablation in hypertensive patients. Heart Rhythm. 2025; 22: 2257-68.
11. Zhang Z, Lin Q, Wang C, Wu K, Huang Y, Tu T, et al. Comparison of Catheter Ablation in Patients with Paroxysmal Non-valvular Atrial Fibrillation and Heart Failure with Preserved Ejection Fraction. Int J Med Sci. 2025; 22: 371-82.
12. Mo D, Wang M, Zhang P, Dai H, Guan J. Factors predicting the recurrence of atrial fibrillation after catheter ablation: A review. Heliyon. 2024; 10: e34205.
13. Kornej J, Hindricks G, Shoemaker MB, Husser D, Arya A, Sommer P, et al. The APPLE score: a novel and simple score for the prediction of rhythm outcomes after catheter ablation of atrial fibrillation. Clin Res Cardiol. 2015; 104: 871-6.
14. Winkle RA, Jarman JWE, Mead RH, Engel G, Kong MH, Fleming W, et al. Predicting atrial fibrillation ablation outcome: The CAAP-AF score. Heart Rhythm. 2016; 13: 2119-25.
15. Dretzke J, Chuchu N, Agarwal R, Herd C, Chua W, Fabritz L, et al. Predicting recurrent atrial fibrillation after catheter ablation: a systematic review of prognostic models. Europace. 2020; 22: 748-60.
16. Bisson A, Fawzy AM, El-Bouri W, Angoulvant D, Lip GYH, Fauchier L, et al. Clinical Phenotypes and Atrial Fibrillation Recurrences After Catheter Ablation: An Unsupervised Cluster Analysis. Curr Probl Cardiol. 2023; 48: 101732.
17. Lang RM, Badano LP, Mor-Avi V, Afilalo J, Armstrong A, Ernande L, et al. Recommendations for cardiac chamber quantification by echocardiography in adults: an update from the American Society of Echocardiography and the European Association of Cardiovascular Imaging. J Am Soc Echocardiogr. 2015; 28: 1-39.e14.
18. Calkins H, Hindricks G, Cappato R, Kim YH, Saad EB, Aguinaga L, et al. 2017 HRS/EHRA/ECAS/APHRS/SOLAECE expert consensus statement on catheter and surgical ablation of atrial fibrillation. Heart Rhythm. 2017; 14: e275-e444.
19. Nattel S, Harada M. Atrial remodeling and atrial fibrillation: recent advances and translational perspectives. J Am Coll Cardiol. 2014; 63: 2335-45.
20. Gottlieb LA, Dekker LRC, Coronel R. The Blinding Period Following Ablation Therapy for Atrial Fibrillation: Proarrhythmic and Antiarrhythmic Pathophysiological Mechanisms. JACC Clin Electrophysiol. 2021; 7: 416-30.
21. Pathak RK, Elliott AD, Lau DH, Middeldorp ME, Linz D, Fitzgerald JL, et al. Aggressive Risk Factor Reduction Study for Atrial Fibrillation Implications for Ablation Outcomes: The ARREST-AF Randomized Clinical Trial. JAMA Cardiol. 2025; 10: 1295-304.